Soft X-Ray Magnetic Imaging of Focused Ion Beam Lithographically Patterned Fe Thin Films

P. J. Cook, T. H. Shen[*], and P. J. Grundy

Institute for Materials Research, University of Salford, Salford, M5 4WT, England.

M. -Y. Im, and P. Fischer

Center for X-ray Optics, Lawrence Berkeley National Laboratory, Berkeley CA94720, USA

S. A. Morton, and A. L. D. Kilcoyne

Lawrence Berkeley National Laboratory, 1 Cyclotron Road, Berkeley CA 94720, USA.

Abstract

We illustrate the potential of modifying the magnetic behavior and structural properties of ferromagnetic thin films using focused ion beam "direct-write" lithography. Patterns inspired by the split-ring resonators often used as components in meta-materials were defined upon 15 nm Fe films using a 30 keV Ga+ focused ion beam at a dose of 2×10^{16} ions cm^{-2}. Structural, chemical and magnetic changes to the Fe were studied using transmission soft X-ray microscopy at the ALS, Berkeley CA. X-ray absorption spectra showed a 23 % reduction in the thickness of the film in the Ga irradiated areas, but no change to the chemical environment of Fe was evident. X-ray images of the magnetic reversal process show domain wall pinning around the implanted areas, resulting in an overall increase in the coercivity of the film. Transmission electron microscopy showed significant grain growth in the implanted regions.

---

* Corresponding Author; E-Mail: t.shen@salford.ac.uk

Nanoscale magnetism is currently an important area of research, with the potential to further developments in conventional magnetic storage media and new forms of magneto-electronic devices [1, 2]. Focused ion beam (FIB) lithography is one of many top-down techniques used to fabricate the structures required to study magnetism on the nanometer scale [3-5]. FIB patterning is particularly attractive because of its "direct-write" nature. This mask-less ion irradiation patterning process, on a scale of tens of nanometers up to tens of microns, is often much faster than other multi-step lithographic techniques.

Ga ion irradiation is known to affect the magnetic properties of ferromagnetic films and in some circumstances render them non-magnetic [6-9], i.e. at high doses or where alloying of multilayered films occurs. Ozkaya *et. al.* show that a Ga ion dose of 1×10^{16} ions cm^{-2} implanted into 30 nm $Ni_{81}Fe_{19}$ films significantly changes the magnetic behavior of the material, increasing its coercivity [6]. This was mostly attributed to an enlarged lattice parameter within the irradiated areas, increasing strain and impeding domain wall movement. Different sputtering rates for the Fe and Ni were seen to alter the composition of the permalloy and was also considered as a possible factor affecting the magnetic behavior. Conversely, Kaminsky *et. al.* reported that Ga implantation into a 15.5 nm $Ni_{80}Fe_{20}$ film with a 9 nm $Ni_{80}Cr_{20}$ capping layer reduced the coercivity, and a dose of 1×10^{16} ions cm^{-2} rendered the film non-ferromagnetic at room temperature [7].

In this paper we present the effects of Ga ion irradiation on the magnetic and structural properties of Fe thin films. Irradiating a ferromagnetic film such as Fe allows us to study the effects of Ga implantation on ferromagnetism without the added complications of differential sputtering and interface mixing that can occur in more complex alloy and multi-layered films.

Several 15 nm Fe films were grown upon 100 nm Si_3N_4 membranes using e-beam evaporation in an ultra high vacuum system. A 30 keV Ga+ FIB was then used to create 40×40 μm^2 patterned areas by irradiating the films with an ion dose of 2×10^{16} ions cm^{-2}. A section of the pattern design is shown in Fig. 1 (c), where the dark areas represent the irradiated material.

Surrounding each pattern is a 1 μm wide frame, also irradiated with a dose of 2×10^{16} ions cm^{-2}. The patterned areas consist of arrays of 'split-ring resonators', the components that are often used to give rise to the negative magnetic permeability in meta-materials [10]. Such a pattern was chosen not only because of the interesting domain structure it may produce, but also to illustrate the versatility of the FIB and highlight its potential within the field of meta-material research. Following the patterning process, the effects of the Ga ion irradiation on the magnetic and structural properties were studied using the full field transmission soft X-ray microscope (XM-1) at beamline 6.1.2 and the scanning transmission X-ray microscope (STXM) (beamline 5.3.2) at the Advanced Light Source (ALS), Berkeley CA. respectively. X-ray magnetic circular dichroism contrast provided detailed images of the magnetic domain structure with XM-1, while the STXM was used to obtain spatially and energy dependent X-ray absorption spectra (XAS) of the patterned surface [11]. Structural changes to the Fe were also studied using transmission electron microscopy (TEM).

XM-1 is a full-field soft X-ray microscope where Fresnel zone plate optics provide a spatial resolution down to 15 nm [12, 13]. It is capable of providing magnetic and element specific information by tuning the photon energy to one of the specimen characteristic absorption edges. Using circularly polarized light emitted off-orbit from a bending magnet source to illuminate the sample through a condenser-pinhole combination, one utilizes X-ray magnetic circular dichroism (XMCD), i.e. the effect that the X-ray absorption coefficient of a ferromagnetic material depends strongly upon the projection of its magnetization onto the helicity of the circularly polarized photons [14]. For Fe, we use an X-ray energy of 707 eV, corresponding to the L_3 absorption edge. The Fe films have an in-plane anisotropy, therefore they are oriented such that the normal of the film surface makes an angle of approximately 30 degrees with the incoming photon beam [15]. This ensures that magnetic contrast can be observed between areas of the film with oppositely oriented components of magnetization that are aligned along the photon propagation direction. An external magnetic field was applied in-plane to saturate the film, then reversed from zero in discrete

steps until saturation was achieved in the opposite direction. A high resolution Fresnel zone plate objective lens generated a magnified image of the film that was projected onto a soft X-ray sensitive CCD at each field step, thus capturing a sequence of the magnetization reversal process. The process was then repeated in the opposite direction, returning the film to its original saturated state. The magnetic domain information shows up on the recorded images as additional contrast superimposed upon the structural information. By calculating the ratios between consecutive images, the structural contrast cancels out, leaving only magnetic information. It is then possible to observe the changes occurring to the domain structure between each of the field steps. This technique has been used to create the sequences in Fig. 1 (a) and (b), in which the magnetization cycle of a small section of the patterned film is shown. An outline of the pattern has been overlaid in each of the images to show the relationship between the structure of the film and the domain formation. The images (i) to (vii) in Fig. 1 (a) show the areas of the film that switch at the applied fields of -53, -119, -148, -170, -203, -225 and -261 Oe, visible as dark regions. It is worth clarifying here that the images are not raw images, but ratios of consecutive images from the original sequence, i.e. only the changes in the magnetization structure show up. For example, image (i) is the ratio between the original image recorded at -53 Oe and the image that precedes it, recorded at zero field. Consequently, only the changes in magnetic signal between these two field values are visible, i.e. only the areas that switch at -53 Oe. Fig. 1 (b) shows the second part of the cycle, where the images (i) to (vi) show the parts of the film switching at the applied fields of 60, 119, 159, 178, 211 and 243 Oe, visible as lightly shaded areas. It is immediately apparent that the Ga irradiation has not dramatically altered the ferromagnetic nature of the film, as the domains are not confined to the Fe rings but are still able to form within the irradiated areas. There is, however, a clear pinning effect created by the implanted features. This is particularly noticeable along the implanted frame that runs approximately parallel to the applied field. This is the last section of the film that is seen to reverse its magnetization in Fig. 1 (a), image (vi) and (b), image (v), at applied

fields of -225 Oe and +211 Oe. It serves to isolate the pattern from the surrounding Fe film outside of the implanted area, the majority of which switches during the first field step, just visible in the lower left corners of the first images in Fig. 1 (a) and (b). Within the pattern itself, the shape of the Fe rings dictates the magnetic reversal. Domains form within the lengths of Fe that lie along the applied field direction, often restricted vertically by the pinning effect of the Fe-Ga. Along the applied field direction however, the pinning is not strong enough to prevent the domains from forming between the rings. It is not clear from observing selected areas of the pattern whether the Fe-Ga is magnetically harder than the as-grown Fe, since in some areas both are seen to switch at the same field. It is clear however, that the implanted regions impede the domain propagation, thus resulting in an increased coercivity when observing the patterned area as a whole.

In principle, the variations in the pixel value (proportional to the transmitted intensity) at a given location throughout the original image sequence represents a magnetic hysteresis loop, characterizing the switching behavior of the corresponding area of the film [13]. In order to plot the hysteresis loops, it was found necessary to correct for intensity variations across the field of view as well as from the gradually decreasing photon beam intensity, and random image shifts up to several pixels between individual frames. We therefore introduce a simple a*d hoc* correction method using image processing software "ImageJ" [16]. The first and last images in the sequence correspond to a magnetically fully saturated Fe film, so the ratio between these two images represents only the change in beam intensity, not part of the magnetic signal. This change is known to be approximately linear over the length of time taken to record the sequence, so we may interpolate the beam intensity for each of the intermediate images. Each image is then normalized to these calculated intensities.

Using the corrected images, a base image is created by calculating the average of the two images recorded at opposing maximum fields, where the film is fully saturated. The pixel values from small sections of Fe and Fe-Ga (indicated on Fig. 2 (a)) were measured throughout the

sequence in order to observe the change in intensity with applied field and plotted as a fraction of the base image intensity in Fig. 2. During the sweep from 0 Oe to -884 Oe, the Fe-Ga requires one more field step than the neighboring Fe area to reverse its magnetization. This indicates restricted domain movement within this sampled area of Fe-Ga and could be a result of morphological changes and damage induced by the Ga implantation. Inset (b) shows the XAS taken from similar areas of Fe and Fe-Ga, which indicates that approximately 23 % of the 15 nm Fe film has been sputtered away in the irradiated areas. For both the Fe and Fe-Ga, the L_2 and L_3 absorption edges occur at 721 eV and 708 eV respectively. There is no apparent change in peak shape or shifting of the absorption edges within the irradiated areas, indicating that the Ga has had no noticeable effect upon chemical environment of the Fe.

TEM images comparing the structure of irradiated Fe to that of as-grown Fe are shown in Fig. 3. The grains were found to be around 25 nm in the Fe areas and 65 nm in the Fe-Ga. The difference in size is clearly visible in Fig. 3 (a), in which sections of Fe and Fe-Ga are shown. When comparing the Fe and Fe-Ga diffraction patterns in Fig. 3 (b) and (c), the difference in grain size is again evident, where the (110) reflection produced by the Fe-Ga is more discontinuous and brighter, indicative of larger grains and possible texturing. The calculated lattice parameters obtained from these rings are 0.286 nm and 0.283 nm for the Fe and Fe-Ga, respectively. This small decrease in lattice parameter is not significantly greater than the experimental error that could be expected in recording the diffraction patterns, but may also relate to a deviation from Vegard's law.

The increase in grain size within the implanted region is a result of the hundreds of displaced Fe atoms per incident Ga ion, creating an ion-induced annealing effect. Using the "SRIM-2008" software, it is possible to simulate the final ion distribution and kinetic phenomena involved during the ion implantation process [17]. The simulation estimates around 700 Fe displacements per Ga ion, so with the high ion dose used here, each Fe atom may have been

displaced many times over. The final ion distribution shows that approximately 60 % of the Ga ions stop within the Fe, with the peak concentration at a depth of around 10 nm. On average, Ga is estimated to constitute approximately 12 % to the film in the irradiated areas.

To summarize, implanting a 15 nm Fe film with 30 keV Ga+ ions at a dose of 2×10^{16} ions cm^{-2} significantly alters its magnetic behavior. Within the patterned area of the film, the domain formation during the magnetization reversal is affected by the magnetostatic energy of the Fe rings, where it is energetically favorable for the domains to form within the longer sections parallel to the applied field. This effect would be more readily seen in a simpler pattern such as a grid; we will be addressing this further in future work. The presence of the Fe-Ga hinders the domain propagation by providing pinning sites for the domain walls leading to an increase in coercivity within the patterned area. Since XAS showed no observable change to the chemical environment of the Fe within the irradiated areas, the domain pinning may be a result of the 23 % reduction in film thickness or significant enlargement of the Fe grains.

References

1. Z. Z. Bandic, E. A. Dobisz, T. W. Wu and T. R. Albrecht, Solid State Technol. **49** (9), S7 (2006).

2. C. A. F. Vaz, T. J. Hayward, J. Llandro, F. Schackert, D. Morecroft, J. A. C. Bland, M. Kläui, M. Laufenberg, D. Backes, U. Rüdiger, F. J. Castano, C. A. Ross, L. J. Heyderman, F. Nolting, A. Locatelli, G. Faini, S. Cherifi and W. Wernsdorfer, J. Phys. –Condes. Matter **19** (25), (2007).

3. J. Fassbender, J. McCord, J. Magn. Magn. Mater. **320** (3-4), 579-596 (2008).

4. G. J. Kusinski, K.M. Krishnan, G. Denbeaux, G. Thomas, B.D. Terris, and D. Weller, Appl. Phys. Lett., **79** (14), 2211-2213 (2001).

5. G. A. Prinz, Science **282**, 1660-1663 (1998).

6. D. Ozkaya, R. M. Langford, W. L. Chan and A. K. Petford-Long, J. Appl. Phys. **91** (12), 9937-9942 (2002).

7. W. M. Kaminsky, G. A. C. Jones, N. K. Patel, W. E. Booij, M. G. Blamire, S. M. Gardiner, Y. B. Xu and J. A. C. Bland, Appl. Phys. Lett. **78** (11), 1589-1591 (2001).

8. N. Owen, H. Y. Yuen and A. Petford-Long, IEEE Trans. Magn. **38** (5), 2553-2555 (2002).

9. R. Hyndman, P. Warin, J. Gierak, J. N. Chapman, J. Ferré, J. P. Jamet, V. Mathet, C. Chappert, J. Magn. Magn. Mater. **240** (1-3), 50-52 (2002).

10. C. M. Soukoulis, S. Linden, M. Wegener, Science **315**, 47-49 (2007).

11. A.L.D. Kilcoyne, T. Tyliszczak, W. Steele, S. Fakra, P. Hitchcock, K. Franck, E.H. Anderson, B. Harteneck, E.G. Rightor, G.E. Mitchell, A.P. Hitchcock, L. Yang, T. Warwick and H. Ade, J. Synchrotron Radiat. **10** (2), 125–136 (2003).

12. W. Chao, B.H. Harteneck, J.A. Liddle, E.H. Anderson and D.T. Attwood, Nature **435**, 1210 (2005).

13. D. H. Kim, P. Fischer, W. L. Chao, E. Anderson, M. Y. Im, S. C. Shin and S. B. Choe, J.

Appl. Phys. **99** (8), 08H303 (2006).

14. P. Fischer, D.H. Kim, W. Chao, J.A. Liddle, E.H. Anderson, D.T. Attwood, Mater. Today **9** (1-2), 26 (2006).

15. P. Fischer, T. Eimuller, G. Schutz, M. Kohler, G. Bayreuther, G. Denbeaux and D. Attwood, J. Appl. Phys. **89** (11), 7159-7161 (2001).

16. W. S. Rasband, ImageJ, U. S. National Institutes of Health, Bethesda, Maryland, USA, http://rsb.info.nih.gov/ij/, 1997-2008.

17. J. F. Ziegler, SRIM-2008, http://www.srim.org

Captions

Figure 1.   Magnetization reversal cycle of a section of patterned Fe, with the applied field in the horizontal direction. The images show the change in domain structure between successive field steps, with an overlay of the pattern design as a guide. The field values between which the changes occur are shown on each image in Oe. An in-plane field of +913 Oe was first applied to saturate the film, then swept from zero field to -884 Oe (a), and then zero field to +913 Oe (b). The pattern design is shown in (c), with the dark areas representing the Ga implantation.

Figure 2.   Partial magnetic hysteresis loops from the two sections of the film highlighted in (a). The dashed lines are present only as guides for the eye and do not represent actual data. (b) X-ray absorption spectra showing the L_2 and L_3 absorption peaks for the Fe and Fe-Ga. The weaker absorption in the Fe-Ga region indicates a reduction in film thickness of 23 %.

Figure 3.   (a) TEM image showing the effect of Ga irradiation on the grain size of the Fe. The grains in the as-grown and irradiated Fe measure approximately 25 nm and 65 nm respectively. Selected area diffraction patterns from the Fe (b) and Fe-Ga (c) show the (110), (200) and (211) rings.
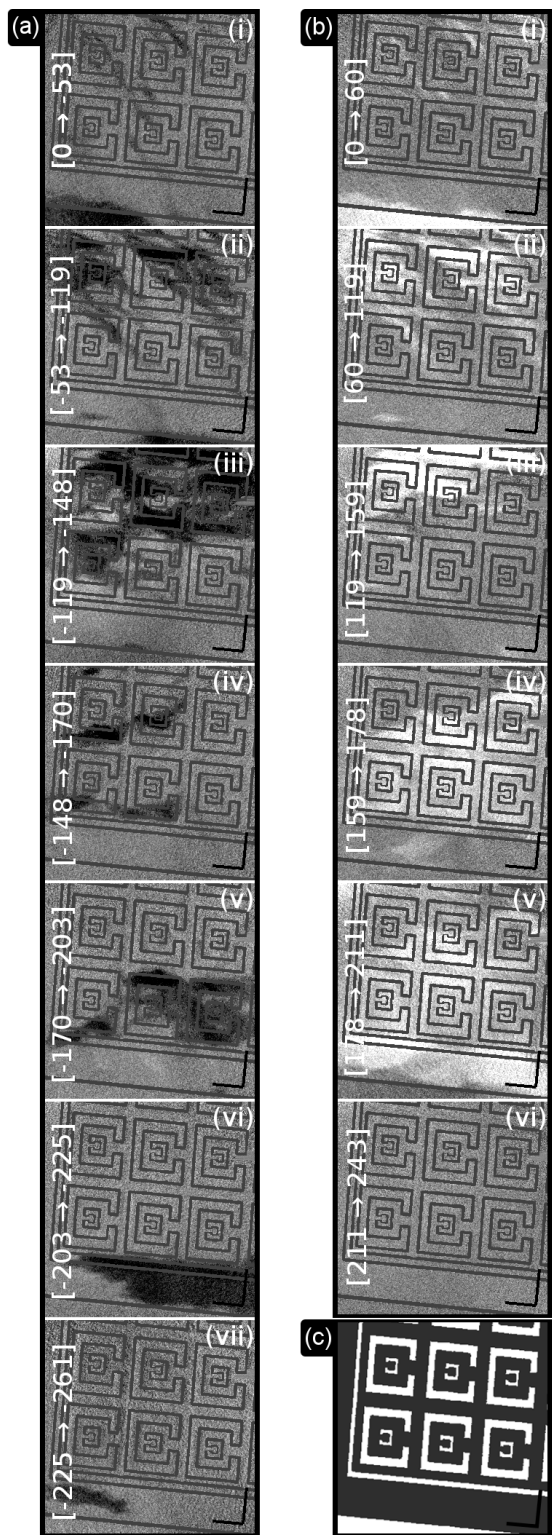
Fig. 1